


J. S. Redinha  
J. da Providência  
A. J. C. Varandas  
Editors



Quantal Aspects  
in Chemistry and Physics

*A tribute to the memory of  
Professor Couceiro da Costa*

## 7. THE QUANTUM ASPECTS OF PROTEINS AND THEIR BIOLOGICAL FUNCTION

H. G. Bohr\*

Quantum Protein (QuP) Center, Technical University of Denmark (DTU),  
Department of Physics, DK-2800 Kgs. Lyngby, Denmark

Peptides, proteins, and especially enzymes, are studied with respect to their quantum behavior which includes electronic states, vibronic states involving the coupling of nuclear and electron motions, excited electronic state dynamics, electron and nuclear tunneling phenomena, bio-Auger processes, charge-density fluctuations and general charge transfer. All these issues are elucidated by quantum electronic calculation of vibrational spectra for small peptides in water solutions, for nucleic acids and finally for protein illustrated by the particular cases of the gene repair processes involving the peptides and then the proteins: Photolyase and Peridinin/ chlorophyll which, respectively, repair UV-radiation damages on genes and harvest light. In the latter two cases the quantum phenomena, such as bio-Auger, are playing a big role.

### 7.1 Introduction

Vibrational spectroscopies, *e.g.*, vibrational absorption (VA), vibrational circular dichroism (VCD), Raman scattering, and Raman optical activity (ROA), have many virtues, including many of the following: being easily accessible (FT IR/VA and FT Raman instruments are now common in most biospectroscopy laboratories, along with the chiral analogues FT VCD and FT ROA), being non-invasive techniques, being able to be measured on a solution and hence one is able to treat solvent effects and observe the biomolecules in their native or near-native environment, and finally with the addition of colloidal particles, as in SERS, it can detect nano-molar quantities which virtually are single molecules or singular

---

\*Email address: hgbohr@gmail.com

molecular complexes or singular molecular machines in dilute solutions [1–3].

However, the difficulty has been to derive theoretical vibrational spectra from quantum electronic calculations in the case of large molecules with more than 10 atoms in their native or near-native environments. This is due to all the couplings between the involved bonds between the atoms. The vibrations basically all couple to each other and this creates a complex picture of superposition of vibrational modes that are hard to interpret and especially if one has to take into account the harmonic and anharmonic couplings with the solvent.

Another problem is that of the large number of conformational states or conformers (as one calls the stable conformations) which appear during the molecular dynamics simulations of peptides (the time scale during with the experiments are being made). These problems, however, open great opportunities in time-resolved spectroscopy since conformational changes can be monitored in time-resolved fluorescence and VA spectroscopy down to the time-scale of nano seconds.

## **7.2 Quantum analysis of small peptides**

We shall firstly present how to use the quantum mechanical calculations of the electronic structures and properties of biomolecules and biomolecular complexes, especially peptides in their native environments, to interpret and understand vibrational spectra and changes in the vibrational spectra either as a reaction proceeds, or in response to a perturbation. From calculated structures and selected molecular properties, the vibrational absorption (VA) and vibrational circular dichroism (VCD) can be simulated from *first principles* within the mechanical harmonic approximation for the vibrational frequencies and normal modes, the electronic harmonic approximation for the electric dipole moments and their derivatives with respect to the nuclear displacements (the atomic polar tensors, APT), and beyond the Born-Oppenheimer approximation for the magnetic dipole transition moments and their derivatives with respect to the nuclear velocities (the atomic axial tensors, AAT). For amino acids, peptides and polypeptides solvent and environmental effects have been shown to affect even

the stability of the conformational states and species present. In addition, the changes which occur as one perturbs a system can be monitored and followed in time with time resolved vibrational spectroscopy. But to do so requires one to be able to reliably take into account the effects of the aqueous environment. These effects have been shown to stabilize both species (the zwitterionic form of amino acids) and conformers, the  $P_{II}$  conformational state of the L-alanine dipeptide (N-acetyl L-alanine N'-methylamide, NALANMA), which are not stable in the isolated state (as single molecular species) in the gas phase or in non-polar solvents. Hence it is fundamental to include explicit water molecules and any other species which are in the first solvation shell (hydration) layer and are responsible for stabilizing the biomolecular complex, the species of interest, and not the so-called isolated biomolecule. Hence not single molecule, but biomolecular complex, or better biomolecular machine or catalyst. Next we present two illustrative cases of our methodology applied to large biomolecules.

The 3 molecules we chose in which to illustrate the types of problems that can arise and how one can overcome/solve there problems are 1. L-alanine (LA); 2. the di-peptide, L-alanyl L-alanine (LALA); and 3. the L-alanine dipeptide, N-acetyl L-alanine N'-methylamide (NALANMA).

In the following sections we present a brief discussion of each molecule and why it is important. This is followed by the most commonly used methodology for simulating vibrational spectra using density functional theory (DFT). The methodology of how one actually can simulate the VA and VCD spectra is presented, followed by a summary of our work which documents and shows the usefulness of our methodology to solve real life structural and functional problems in molecular biophysics and molecular biology.

### **7.2.1 L-alanine**

L-alanine (LA) is the simplest chiral amino acid with the methyl group replacing one of the two achiral hydrogens in glycine. All other amino acids are more complicated. The chiral nature of 19 of the 20 naturally occurring amino acids gives the preference for right handed  $\alpha$  helices over the left hand variant

in peptides and proteins. In addition, the preference of the so-called  $C_7^{eq}$  conformer over the so-called  $C_7^{ax}$  conformer for small peptides is due to the bulky  $C_\beta$  group of the 19 chiral amino acids. Here we focus initially on the various possible species of the L-alanine in aqueous solution, its native environment, at neutral pH. In the isolated single molecular state in either the gas phase or in non-polar solvents like carbon tetrachloride or carbon disulfide, the species of L-alanine present is the non-ionic neutral species,  $\text{NH}_2 - \text{CH}(\text{CH}_3) - \text{COOH}$ , while in aqueous solution the species present is the ionic neutral species, the so-called zwitterionic species,  $\text{NH}_3^+ - \text{CH}(\text{CH}_3) - \text{COO}^-$ . We and others have shown that to correctly simulate and interpret the VA, VCD, Raman and ROA spectra of the zwitterionic form of LA in aqueous solution, one must include explicit water molecules [4–9]. Hence the molecule or molecular complex of interest is not the individual single molecule, but the hydrated zwitterionic species. Which and how many of the water molecules are not only important, but an integral part of the species of interest is the more relevant question.

### 7.2.2 L-alanyl L-alanine

On peptide formation, two amino acids interact chemically to form a peptide bond. The species present in aqueous solution at neutral pH is again the ionic neutral zwitterionic species, and not the nonionic species present as a isolated single molecule either in the gas phase or in nonpolar solvents. Here, once again, the species of interest is stabilized by the presence of a finite number of strongly interacting water molecules of the aqueous environment. The isolated single molecular state in either the gas phase or in non polar solvents is the non-ionic neutral species,  $\text{NH}_2 - \text{CH}(\text{CH}_3) - \text{CO} - \text{NH} - \text{CH}(\text{CH}_3) - \text{COOH}$ .

To simulate the aqueous environment, we initially added a small number of explicit water molecules to stabilize the zwitterionic species of the L-alanyl L-alanine (LALAZ) [4], but subsequently used classical molecular dynamics simulations of LALAZ in a box of water molecules to determine the number and positions of the water molecules in the so-called first solvation shell of water molecule encapsulating and stabilizing the LALAZ. We initially kept only those

water molecules which were directly interacting with the polar and ionic groups of the LALAZ via hydrogen bonding and subsequently performed geometry optimizations [10]. For one of these optimized structures, we performed a Hessian calculation and subsequently APT and AAT which allowed us to simulate both the VA and VCD spectra. Finally we also used Gaussian and CADPAC to calculate the tensors necessary for us to simulate the Raman and ROA spectra, that is the various polarizability derivatives, all at the restricted Hartree-Fock (RHF) level of theory [11].

In this work we extend that work by increasing the number of water molecules interacting with the LALAZ and, in addition, use DFT polarizability derivatives, which have been shown to be in general more accurate than those calculated at the RHF level of theory. For the di-peptide zwitterion, LALAZ, we have simulated the VA and VCD spectra in aqueous solution. The LALAZ molecular complex has 23 atoms in addition to the 14, 17 and 40 water molecules which we have used to solvate the LALAZ. This case represents a quite formidable task for a complete quantum mechanical calculations of the VA, VCD, Raman and ROA spectra in a native aqueous environment.

For simple energy only calculations, the LALAZ may be a relatively small molecule, but for calculation of the dynamical nature of the solvent shell of water molecules and the molecular properties for the LALAZ, one requires a larger basis set and more sophisticated methods than one normally uses for the former case. For the case of individual single isolated state molecules, one can normally use the PM6 and SCC-DFTB or SCC-DFTB+Disp semi-empirical based wave function and density functional theory methods. But these methods do not allow one to calculate the tensors required for VCD, the AAT, and the ROA, electric dipole-magnetic dipole polarizability derivatives (EDMDPD) and the electric dipole-electric quadrupole polarizability derivatives (EDEQPD), in addition to the APT and the electric dipole-electric dipole polarizability derivatives (EDEDPD) which are required for the VA and Raman spectral simulations.

### 7.2.3 N-acetyl L-alanine N'-methylamide

When one forms a tri-peptide, one for the first time introduces the so-called  $\phi$  and  $\psi$  angles, which determine uniquely the backbone structure for peptides, polypeptides and proteins. Rather than deal with these two backbone angles and additionally, the zwitterionic species, we and many others have decided to cap the ammonium group with the N-acetyl group to form a peptide group at the N-terminal and cap the carboxylate group with the N'-methylamide group to form a second peptide group at the C-terminal: N-acetyl AA N'-methylamide dipeptide.

The most recent works where we have given a very thorough review of the existing literature on NALANMA and the problem which we addressed, that is, what structural changes in NALANMA are responsible for the large changes seen in the VA, VCD, Raman and ROA spectra when one changes from either an inert gas matrix or nonpolar solvent, to aqueous solution [4, 9, 12–15]. Here we and others have found that the conformer present in aqueous solution, the  $P_{II}$  conformer, is not stable in the nonpolar solvents or at low temperature in inert gas matrices [4, 9, 12–14, 16, 17]. In addition, it has recently been found that some of the positions of the bound waters of biomolecules actually are stable on the time scale of the VA and VCD spectra and actually have been shown to possess a chiral character [18], further documenting and supporting our paradigm that explicit water molecules are an inherent part of the structure, and in many cases of function, of biomolecules in their native environment.

### 7.2.4 Materials and methods

At the various optimized geometries various zwitterionic species stabilized by varying numbers of water molecules form biological complexes which have been embedded within the Onsager, PCM, CPCM and COSMO continuum models. Hessian and atomic polar tensor (APT) (Amos 1984) [19] and atomic axial tensor (AAT) calculations with Gaussian 94, 98 and 03. Restricted Hartree-Fock (RHF) atomic axial tensor (AAT) (Stephens 1985, 1987 [20, 21]; Buckingham *et al.* 1987 [22]; Amos *et al.* 1987 [23]) calculations have also been performed util-

izing the Cambridge Analytical Derivatives Package (CADPAC) Issue 5.2, 6.0 - 6.3. These calculations were performed utilizing the distributed origin gauge (Stephens 1987 [21]; Amos *et al.* 1988 [24]) and restricted Hartree-Fock (RHF) wave functions. Coupled Hartree-Fock theory has been utilized for the Hessian, APT and AAT calculations [25]. The AAT tensors have also been implemented in Gaussian 98 by Cheeseman *et al.* 1996 [26]. The AAT have also been derived such that they can be calculated by a sum over states methodology [27] and have been implemented in the SYSYM suite of programs by Lazzaretti and Zanasi [28]. The AAT tensors have also been implemented at the MCSCF level by Bak *et al.* 1993 [29,30]. The EDEDPD have been implemented at the RHF and DFT level [31–34]. These are the tensors which are needed to predict the Raman intensities. In addition to these tensors, one requires the EDEQPD and the EDMDPD. The EDEQP and EDMDP have been implemented at the RHF level and more recently the EDMDP have also been implemented at the DFT level [35–38]. The DFT EDMDP have also been recently used to calculate the optical rotation for a number of molecules [39]. Recently much work has appeared at the DFT and other correlated levels to calculate the static and frequency dependent polarizabilities and hyperpolarizabilities [40–47].

## VA calculations

The Hessian and APT calculations were performed using the 6-31G\* basis set with Gaussian 94, 98 and 03. The vibrational absorption spectra is related to molecular dipole strength via

$$\epsilon(\bar{\nu}) = \frac{8\pi^3 N_A}{3000bc(2.303)} \sum_i \bar{\nu} D_i f_i(\bar{\nu}_i, \bar{\nu}), \quad (7.1)$$

where  $\epsilon$  is the molar extinction coefficient,  $D_i$  is the dipole strength of the  $i$ -th transition of wavenumbers  $\bar{\nu}_i$  in  $\text{cm}^{-1}$ ,  $f(\bar{\nu}_i, \bar{\nu})$  is a normalised line-shape function, and  $N_A$  is Avogadro's number.

For a fundamental (0→1) transition involving the  $i$ -th normal mode within



the harmonic approximation

$$D_i = \left( \frac{\hbar}{2\omega_i} \right) \sum_{\beta} \left( \sum_{\lambda\alpha} S_{\lambda\alpha,i} \mu_{\beta}^{\lambda\alpha} \right) \left( \sum_{\lambda'\alpha'} S_{\lambda'\alpha',i} \mu_{\beta}^{\lambda'\alpha'} \right), \quad (7.2)$$

where  $\hbar\omega_i$  is the energy of the  $i$ -th normal mode, the  $S_{\lambda\alpha,i}$  matrix interrelates normal coordinates  $Q_i$  to Cartesian displacement coordinates  $X_{\lambda\alpha}$ , where  $\lambda$  specifies a nucleus and  $\alpha = x, y$  or  $z$ :

$$X_{\lambda\alpha} = \sum_i S_{\lambda\alpha,i} Q_i. \quad (7.3)$$

$\mu_{\beta}^{\lambda\alpha}$  ( $\alpha, \beta = x, y, z$ ) are the APT of nucleus  $\lambda$ .  $\mu_{\beta}^{\lambda\alpha}$  are defined by

$$\mu_{\beta}^{\lambda\alpha} = \left( \frac{\partial}{\partial X_{\lambda\alpha}} \left\langle \psi_G(\tilde{R}) | (\mu_{el})_{\beta} | \psi_G(\tilde{R}) \right\rangle \right)_{\tilde{R}_0} \quad (7.4)$$

$$\mu_{\beta}^{\lambda\alpha} = 2 \left\langle \left( \frac{\partial \psi_G(\tilde{R})}{\partial X_{\lambda\alpha}} \right)_{\tilde{R}_0} \mid (\mu_{el}^e)_{\beta} \mid \psi_G(\tilde{R}_0) \right\rangle + Z_{\lambda} e \delta_{\alpha\beta}, \quad (7.5)$$

where  $\psi_G(\tilde{R})$  is the electronic wavefunction of the ground state G,  $\tilde{R}$  specifies nuclear coordinates,  $\tilde{R}_0$  specifies the equilibrium geometry,  $\tilde{\mu}_{el}$  is the electric dipole moment operator,  $\tilde{\mu}_{el}^e = -e \sum_i \tilde{r}_i$  is the electronic contribution to  $\tilde{\mu}_{el}$  and  $Z_{\lambda} e$  is the charge on nucleus  $\lambda$ .

### VCD calculations

The vibrational circular dichroism spectra is related to the molecular rotational strengths via

$$\Delta\epsilon(\bar{\nu}) = \frac{32\pi^3 N}{3000bc(2.303)} \sum_i \bar{\nu} R_i f_i(\bar{\nu}_i, \bar{\nu}), \quad (7.6)$$

where  $\Delta\epsilon = \epsilon_L - \epsilon_R$  is differential extinction coefficient,  $R_i$  is the rotational strength of the  $i$ -th transition of wavenumbers  $\bar{\nu}_i$  in  $\text{cm}^{-1}$ ,  $f(\bar{\nu}_i, \bar{\nu})$  is a normalised line-shape function, and  $N_A$  is Avogadro's number.

$$R_i = \hbar^2 \text{Im} \sum_{\beta} \left( \sum_{\lambda\alpha} S_{\lambda\alpha,i} \mu_{\beta}^{\lambda\alpha} \right) \left( \sum_{\lambda'\alpha'} S_{\lambda'\alpha',i} m_{\beta}^{\lambda'\alpha'} \right), \quad (7.7)$$

where  $\hbar\omega_i$  and the  $S_{\lambda\alpha,i}$  matrix are as previously defined.  $\mu_{\beta}^{\lambda\alpha}$  and  $m_{\beta}^{\lambda\alpha}$  ( $\alpha, \beta = x, y, z$ ) are the APT and AAT of nucleus  $\lambda$ .

$\mu_\beta^{\lambda\alpha}$  is as previously defined and  $m_\beta^{\lambda\alpha}$  is given by

$$m_\beta^{\lambda\alpha} = I_\beta^{\lambda\alpha} + \frac{i}{4\hbar c} \sum_\gamma \epsilon_{\alpha\beta\gamma} R_{\lambda\gamma}^0(Z_\lambda e) \quad (7.8)$$

$$I_\beta^{\lambda\alpha} = \left\langle \left( \frac{\partial \psi_G(\tilde{R})}{\partial X_{\lambda\alpha}} \right)_{\tilde{R}_e} \left| \left( \frac{\partial \psi_G(\tilde{R}_e, B_\beta)}{\partial B_\beta} \right)_{B_\beta=0} \right. \right\rangle, \quad (7.9)$$

where  $\psi_G(\tilde{R}_0, B_\beta)$  is the ground state electronic wavefunction in the equilibrium structure  $\tilde{R}_e$  in the presence of the perturbation  $-(\mu_{mag}^e)_\beta B_\beta$ , where  $\tilde{\mu}_{mag}^e$  is the electronic contribution to the magnetic dipole moment operator [20, 22].  $m_\beta^{\lambda\alpha}$  is origin dependent. Its origin dependence is given by

$$(m_\beta^{\lambda\alpha})^0 = (m_\beta^{\lambda\alpha})^{0'} + \frac{i}{4\hbar c} \sum_{\gamma\delta} \epsilon_{\beta\gamma\delta} Y_\gamma^\lambda \mu_\alpha^{\lambda\delta}, \quad (7.10)$$

where  $\tilde{Y}^\lambda$  is the vector from O to O' for the tensor of nucleus  $\lambda$  [21, 24, 48]. Equation (10) permits alternative gauges in the calculation of the set of  $(m_\beta^{\lambda\alpha})^0$  tensors. If  $\tilde{Y}^\lambda = 0$ , and hence O = O', for all  $\lambda$  the gauge is termed the Common Origin (CO) gauge. If  $\tilde{Y}^\lambda = \tilde{R}_\lambda^o$ , so that in the calculation of  $(m_\beta^{\lambda\alpha})^0$  O' is placed at the equilibrium position of nucleus  $\lambda$ , the gauge is termed the DO gauge (Stephens 1987 [21]; Jalkanen 1988 [48]; Amos *et al.* 1988 [24]). Density functional theory atomic axial tensors have also been implemented in Gaussian 94 (Cheeseman *et al.* 1996) [26]. We have utilized Gaussian 98, 03 to calculate the AAT used in this work.

## QM methods

The B3LYP hybrid exchange-correlation functional method is a hybrid DFT method where the exchange-correlational (XC) functional has been parameterized to reproduce experimental data. The parameter values were specified by Becke by fitting to atomization energies, ionization potentials, proton affinities and first-row atomic energies in the G1 molecule set [49–54]. Recently, Frish and coworkers showed that the B3LYP/6-31G\* method accurately reproduce gas phase and nonpolar solution geometries, vibrational frequencies and absorption, and vibrational circular dichroism (VCD) intensities [13]. This level of theory has been documented to model structures and VA spectra of NALANMA, LA and

LALA in aqueous solution by adding explicit waters to take into account the first solvation shell which strongly interact with the peptide as well as the Onsager continuum model added to take into account the interaction of the peptide with bulk water [5, 10, 11, 14]. At this level of theory, we are confident in that many properties of interest for small peptides, i.e., structural parameters, vibrational frequencies, and relative VA intensities can be accurately modelled.

## **7.2.5 Results and discussion about the peptide calculation**

### **Structures of LA, LALA and NALANMA**

The zwitterionic forms of both LA and LALA were only found by including explicit water molecules. The use of the Onsager, PCM and CPCM continuum models were all shown to be inappropriate for taking into account the first solvation shell of water molecules responsible for stabilizing not only the zwitterionic species, but the most stable conformer for each. In the case of the alanine dipeptide, the importance of explicit water molecules was again shown to be fundamental, as the conformer seen in aqueous solution and evidenced by the VA, VCD, Raman, ROA and NMR spectra was that of the conformer which IS NOT STABLE on either the gas phase isolated state potential energy surface or that obtained with one of the three continuum models, be it Onsager, PCM or CPCM. Hence the use of these continuum solvent models for the treatment of first solvation shell water molecules should be DISCONTINUED, and these models should only be used to treat bulk water effects.

### **VA, VCD, Raman and ROA spectra of LA, LALA and NALANMA**

The VA, VCD, Raman and ROA spectra, both experimental and theoretical have been presented in a number of publications now so there is no need to reproduce that data here. The summary is that the VA and VCD or the Raman and ROA spectra alone are not sufficient to answer all structural and functional problems, so that the set of all four spectra should not only be measured, but also simulated. In addition, it also pays to measure the NMR spectra and if possible, also, the inelastic incoherent neutron scattering (IINS) spectra, as the

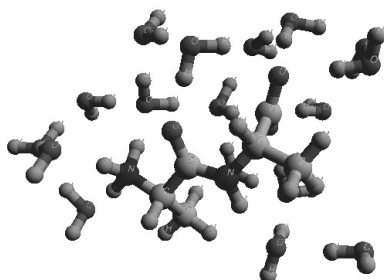


Figure 7.1. L-alanine L-alanine zwitterion plus 17 waters

selection rules for IINS vibrational spectroscopy are fundamentally different than those for VA and VCD or Raman and ROA. A model or paradigm which is not able to reproduce all of the available experimental data is not of much general use. Hence we also advocate measuring not only the conventional VA/IR and Raman, but also the chiral analogues, VCD and ROA, and the IINS vibrational spectra. Recent work by Kearley and coworkers at ANSTO in Australia and Holderna-Natkaniec and coworkers in Poland have shown that this additional data is complementary to that gained from the other spectroscopies [55, 56]. Hudson has also shown that the IINS can be used interpreted using ab initio calculations [57].

In Figure 7.1 we show an ab-initio optimized structure of LALA with 17 water cluster/droplet embedded within the cavity created with the polarized continuum model (PCM) using the B3LYP hybrid exchange correlation functional (DFT) with the 6-31G\* basis set. In Figs. 7.2, 7.3 and 7.4 we show the simulated vibrational absorption (VA), vibrational circular dichroism (VCD) and Raman spectra for the LALA zwitterion in a droplet of 17 water molecules embedded with the PCM cavity.

### 7.2.6 Summary and conclusions of the alanine peptides studies

By analyzing not only the VA, VCD, Raman and ROA spectra of LA, LALA and NALANMA, but also the spectra of the various isotopomers, we have been

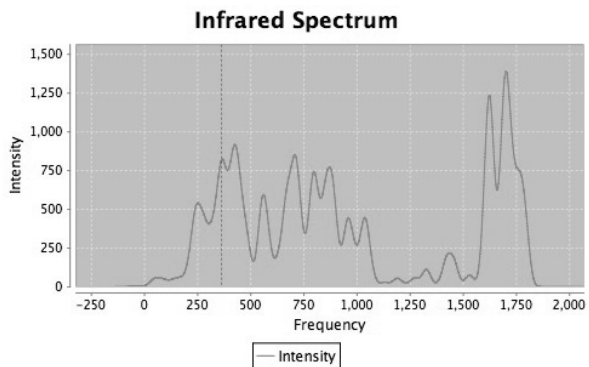


Figure 7.2. Vibrational absorption of L-alanine L-alanine zwitterion plus 17 waters

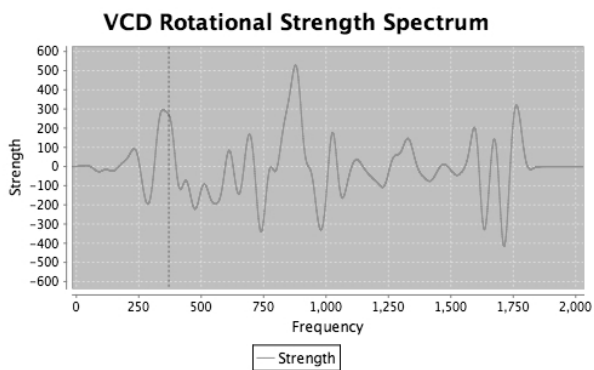


Figure 7.3. Vibrational circular dichroism of L-alanine L-alanine zwitterion plus 17 waters

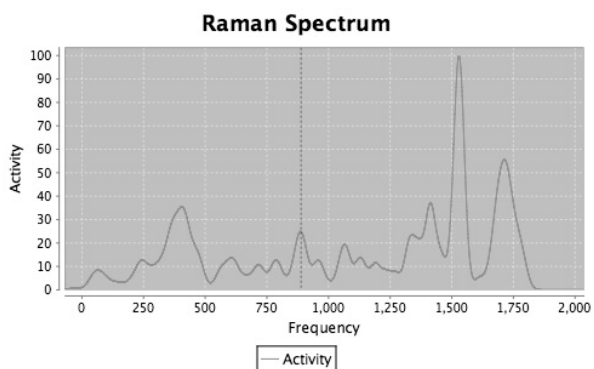


Figure 7.4. Raman spectra of L-alanine L-alanine zwitterion plus 17 waters

able to address the issue raised by Freedman [58, 59] on the previous Raman and ROA simulations for LALA [60]. This work shows that analysis of the isotopic data both experimentally and theoretically is very valuable in verifying the accuracy of both the force field and the various tensor quantities necessary to simulate the VA, VCD, Raman and ROA spectra. The issue of having the correct structure, species and conformer (or conformers) are also important. Our previous works [4–7, 13, 14] have shown that it is very important to take into account the first solvent shell water molecules which are interacting strongly with the solute via H-bonding explicitly. The continuum model can be used to treat the effect due to the bulk water molecules.

To be able to simulate L-alanine in aqueous solution it has been important and fundamental to add explicit water molecules to not only stabilize the zwitterionic species, but to also get the the conformer of the zwitterionic species found in aqueous solution. The simple continuum models and even simple Hartree-Fock theory are in some cases able to get a stable zwitterionic species, but not the variety of conformers stabilized and populated in aqueous solution. Our most recent work shows that to completely solvate the zwitterionic species requires 20 water molecules. The initial placement of the water molecules has been obtained from Born-Oppenheimer DFT molecular dynamics simulations. This is due the problem with classical molecular dynamics models for water failing to reproduce the first hydration layers around biomolecules correctly.

To be able to simulate the alanine dipeptide in aqueous solution has also required one to include the first solvation shell water molecules which actually stabilize a conformer which is not stable in the gas phase. Hence without the explicit water molecules, like in the case of the L-alanine zwitterion, one cannot get the variety of conformers stabilized and populated in aqueous solution. Our new paradigm has solved the problem of what is the stable conformer of the alanine dipeptide in aqueous solution, and WHY. NMR studies have conformed our work and provided even more evidence for the importance of including explicit water molecules not only for simulating the vibrational spectra, but also the NMR spectra, and also function.

Finally to take into account temperature effects, one could consider the use of QM/MM methodology as an alternative to our hybrid model and we are pursuing this methodology also and look forward to presenting our comparison of these two methods in the near future. Here one would run molecular dynamics simulations using high level *ab initio* methods (beyond simple Hartree-Fock) or DFT methods like those being developed in the Bartlett group in Gainesville, Florida, the so-called *ab initio* DFT [61]. Here one uses the accumulated knowledge from wave functional quantum mechanics to develop local exchange and correlation functionals based on the optimized effective potential (OEP) method. Preliminary works by the Bartlett group and many others have shown that this methodology provides a way to systematically improve both exchange and correlation functions. So the so-called Holy Grail of DFT may be found in the not so-distant future, providing a methodology which will allow us to perform ground electronic state Born-Oppenheimer molecular dynamics simulations. This will in theory allow us to do the correct averaging over time to get the conformational fluctuations and even chemical reactions. This will allow us to do quantum nanobiology. Of course the methods will need to be benchmarked, like our work on LA, LALA and NALANMA. Finally the extension to do excited electronic state molecular dynamics simulations will be the next obvious extension. Many groups and researchers are currently working in that field, which is beyond the scope of our work, but we would like to make the readers of this work aware of the extension of this work to that field.

### **7.3 Examples on quantum electronic calculations on protein complexes**

In the following we shall give 2 interesting examples of quantum electronic calculations for proteins in the gene repair processes and for the photosynthesis processes.

#### **7.3.1 Case I: Electronic processes of photolyase protein in gene repair**

This work presents a study on the ground and excited state properties of thymine, thymine dimers and thymine duplex as the work relates to the damage

of nucleic acids and the repair system by DNA photolyase. We especially present our contribution to this problem based on our theoretical simulations. It is also interesting to study the species which are results of the absorption of radiation, the free radicals. In some cases the resulting species is a neutral radical and in other cases a radical cation. We also analyze the mechanisms of DNA damage and radiation mediated DNA repair both from an evolutionary and genetic engineering point of view. The main result of the study is that excited electronic state is a necessary ingredient of the repair process due to the energy balance since it gives means for overcoming the reaction barrier.

### **7.3.2 Introduction to Gene Repair**

The damage of DNA by UV-radiation is a well-known problem which has been studied for some time [68,69]. It appears that the repair mechanism is present in many plants and animals exposed to the damaging radiation. One repair mechanism, which is the focus of this paper, is making use of external blue light for the reactivation but there are other repairs which directly replace the erroneous DNA patch.

Here we would like to study the influence of the wavelength of the radiation on the various chemical and photochemical processes that both lead to the damage, but also that lead and contribute to the repair. Both of these processes seem to have mechanisms (processes) that appear to be photo-activated. The influence of the environment plays an important role in these processes. The mechanism(s) will probably very much depend on what the system is and the environment. Here by system we refer to the object which is interacting with the electromagnetic radiation. The DNA photolyase repair process is here seen as a prime example of a process that only can proceed provided electronic excited states are included in the reaction path.

Normally one must treat this part or entity quantum mechanically. If one uses either visible or ultraviolet radiation as the exciting radiation, one excites an electron in the system to a higher energy level which is not populated in the ground state. Hence we can call the state to which the electron is excited



an excited state. One also has the question as to what is the best or even an adequate level of theory to represent these excited states. Density functional theory as originally formulated is a theory to represent or find the energy for the ground state potential energy surface. Hence we can use it with confidence to follow conformational changes which do not involve the making and breaking of chemical bonds. It can also be used to model chemical reactions, but if the barrier and/or mechanism involves states which can not be represented by a single Slater determinant of either the Hartree-Fock or Kohn-Sham orbitals, then one must be careful in trusting or having confidence in the results. Also the questions of how large a basis set to use, whether one required diffuse and/or polarization orbitals, and how to treat both electron correlations and electron exchange must be dealt with. In the section of this paper which follows, we shall give our overall strategy for approach and the preliminary results we have to date.

In this study we will focus on the damaged thymine molecule and its repaired state. It is the calculation of this molecule that gives results that can lead to new insight into the repair mechanism. The phosphodiester backbone of the DNA molecule and the co-inzyme, flavin, molecule are included as background for the dithymine molecule as well as the photolyase protein.

Let us briefly review what is up to now believed to be the photo-reactivation repair process with photolyase seen from a bio-molecular physics viewpoint. Ultra-violet radiation, particular in the range of 200-300 nm wavelength, irradiated on 2 thymine nucleotides in DNA, creates a dimerization attaching them together, thereby creating a lesion on DNA in the form of a disruption on the helical axis. This lesion perturbs the structure of DNA and leads to an error in the code and causing problems for the transcription [70]. Under photoreactivation in the visible and near UV region (basically just blue light) the defect is repaired, breaking the the new bonds constituting the lesion, and restoring the thymines back to the original state of two separate thymine nucleotides. The photolyase protein and its cofactor, riboflavin FADH, are thought to catalyze the repair process by absorbing light and transferring electrons to the destroyed

DNA patch of dithymine. In the following study we shall be analyzing the repair mechanism and perform electronic quantum calculations on the reaction complex. Firstly, we give an overview of the methodology and of the strategy in the calculations and next we shall, in the subsequent chapter, be giving results of the computer calculations and analyze the data. Finally, we conclude the study.

### **7.3.3 A model for the repair process**

Ultra violet radiation, particularly in the range of 200-300 nm wavelength, irradiated on thymine in DNA, creates a dimerization attaching two of them, thereby creating a kink in the helical axis of DNA. This lesion perturbs the structure of DNA and leads to an error in the code and causing problems for the transcription [71, 72]. Under photo-reactivation in the visible and near UV region the defect is repaired, breaking the lesion and restoring the thymines back to the original state [73].

The whole process is a fascinating one from the energy balance as well as a regenerative repair viewpoint. A mutation caused by electromagnetic (EM) radiation of higher energy is restored to its original structure by exposing the mutant to photons having lower energy. This requires careful development of a theory which addresses the question of the energy conservation in the whole process (see Ref. 70). There have been many investigations studying separately the mechanisms of the absorption of UV radiation and the repair process, but there has, so far, been no report examining both processes taken together. For example, Reuther et al. [74] have done an extensive study on the UV absorption process involved in the aqueous solution of thymine but do not relate the role of these physical properties to the repair mechanism. Similarly, much effort have gone into the study of repair mechanisms, particularly the role of photolyase and DNA [75–77] but no attempt has been made to address the question of imbalance of energy occurring between the mutation and the repair mechanism. In this note, we attempt to analyze the energy and charge balance question and investigate both the mutation and repair processes in a common, quantum physical framework discussed in the next section. The formation of a

meta-stable electronically excited state by absorbing the incident UV radiation via inter-system crossing and its eventual de-excitation by radiationless Auger transition, provide two mechanisms that are compatible with the energy balance in the process. The restoring mechanism of Auger transition, usually being a radiationless phenomenon, cannot cause further radiation damage.

The important question now is to investigate whether an electronic excitation causing a structural change can result into the formation of a dimer. Clearly, 4 to 6 eV energy is insufficient to ionize a thymine, which requires an energy of about 12 eV. The energy associated in splitting a covalent bond between two C, or H – O, or H – C etc. is between 0.59 to 0.8 eV, which is equivalent to 3.67 to 5.00 eV [69]. Certainly, 200 to 300 nm UV radiation is in the position to break many of the covalent bonds that bind to form a thymine. However, the breaking of one or more of these bonds is likely to cause a major disruption to its structure. This would be difficult to reverse by illuminating it with optical radiation which does not simply have enough energy to restore these bonds. For example, optical radiation of 400 and 580 nm has energies of 3.09 and 2.13 eV, respectively, which are significantly below the energy necessary to form these bonds. The problem of the energy imbalance persists in case one of the covalent bonds of a member molecule of a thymine is detached and then attached covalently to another molecule of a different thymine to form a dimer, because the energy difference to these processes is far less than 4 to 6 eV incident energy dumped by UV radiation. This amount of energy cannot simply be argued to be lost in dissipation, because in the process of restoration of a dimer to two detached thymines, the difference of energy between UV and optical radiation must be put back from somewhere causing a change in entropy to be negative, which is against the laws of physics as known. There could of course be extra solvent effects but that will imply a much more complex machinery to restore the dimer in its original state.

The electronic transition from the ground state configuration of thymine to an excited electronic state remains as an alternative. To gain further insight in that possibility, we consider a few diatomic pyrimidine ring components (PRC),

e.g., CH, CO and NH. The ionization potential of these PCR are, respectively, 10.64, 14.01, and 14.1 eV see Ref. 10 making ionization of these PCR energetically impossible. On the other hand, there are many electronic excited states in the energy range of 4 to 6.5 eV in these PCR [70].

### 7.3.4 Overview of strategy

#### ***Ab initio* methods**

The building blocks of DNA are the four base pairs, adenine, thymine, guanine, and cytosine. In RNA uracil replaces thymine. In addition to the four bases, there is also present the five membered deoxyribose (ribose in RNA) carbohydrate and the phosphate moiety. There has been much work on the individual bases and the nucleotides. These results have been at the restricted and unrestricted Hartree-Fock, 2nd order Møller Plesset and DFT levels of theory. For the ground state one can also utilize approximate DFT methods. To be able to understand the photo activated DNA repair via DNA photolyase, then we must also consider the whole mechanism. Recently Sancar has written a 50 year review on enzymatic photo-reactivation [81]. Here he states that his field started in 1949 with the discovery of photo-reactivation by Alfred Kelner [82,83]. Shortly after the seminal work by Kelner, Dulbecco reported the reactivation of ultraviolet exposed bacteriophage, but only when the phage and *E. coli* were together during exposure to the photo-reactivating light [84].

The main focus of our study of the photolyase system is to try to calculate the electronic structure and see if such structure corresponds to the experimental data observed. We have hence made quantum mechanical calculations using the Density Functional Theory (DFT), to obtain electronic structures of part of the protein-DNA-cofactor complex. A big issue have been to extract knowledge about the electronic excited states even though the standard programs are only available at the ground state level.

In the following section we will discuss the *ab initio* and semi-empirical DFT based methods as applied to calculating the ground state properties.

## **Methods for ground state calculations**

Basically the following methods are used for the electronic calculation:

- The Hartree-Fock methods
- The 2nd order Møller Plesset methods
- The density functional method
- The local density approximation
- The generalized gradient approximation in DFT
- The hybrid DFT approximation

We would like to introduce our work on the development of a relatively new semi-empirical method based on an approximation to density functional theory, the so called self consistent charge tight binding method (SCC-DFTB) [85–87]. It had been previously been used in solid state physics, but had not been parameterized for modeling biomolecules. We have previously benchmarked this theory for use in modeling small peptides [15] and small ring systems [88].

## **Methods for excited state calculations**

To treat the excited states one faces additional problems, which do not have to be dealt with when modeling the ground state. One problem involves the optimization of the electronic states. Ordinarily the optimization will relax the electronic state. One can, however, within the standard quantum mechanics “Gaussian” program get a hint about the excited state by looking at the lowest unoccupied electronic orbital (LUMO) and the highest occupied electronic orbital (HOMO) in a quantum mechanical calculation of the electronic system. This is what automatically comes out of the calculation. The only extra thing one will have to do with respect to the excited states, is to carry an electron from the HOMO state to the LUMO state, since this state has no electrons, and take into account that extra energy.

We therefore calculate the HOMO/LUMO state gap for the various ground state structures of the thymine molecules. The energy and occupancy of these states are given for the different structures in Table 1 and 2 of Ref. 78.

A serious objection to just use the LUMO state as an excited state is that it is empty by definition. That is even though the notion of the HOMO/LUMO gap gives us an understanding of the level splitting in energy. This splitting in energy serves the understanding of the basic question of this paper, which is that of energy conservation: "How can a damage caused by UV light be repaired by a process requiring much less energy of blue light. The answer is that by making use of the excited electronic states, the repair processes can circumvent overcoming the large barrier between the ground state of dithymine and bonded duplex of thymine, the latter being the damaged state caused by UV radiation. When calculating the HOMO/LUMO gap and using that as a measure of a relevant energy difference we just have to make sure that the extra energy for an electron present in the LUMO state is negligible compared to the bare HOMO/LUMO gap.

Therefore we should do the calculation again with an electron taken from the HOMO state and put it into the LUMO state. Such calculation can be performed again in the standard DFT calculation programme and the results are presented in reference [78].

### **7.3.5 Empirical computational methods: Molecular mechanics and molecular dynamics for DNA and proteins**

For nucleic acids and proteins molecular mechanics and molecular dynamics methods have been the methods of choice. This is due to the computational cost. These methods are much faster than *ab initio* and even semi-empirical methods. But one must normally have a force field. Here one must choose a functional form and then determine empirical parameters [89]. There has been a whole evolution of force fields and here we will not go into detail into that, since it would require a complete work in itself. But we will describe the history, development and current status as it relates to the work on amino acids and small and intermediate sized peptides. The most commonly used force fields are the Amber force fields [90, 91], the MM4 force fields [92], the Groningen MOlecular Simulation (GROMOS) program package force fields [93, 94], the optimized po-

tentials for liquid simulations (OPLS) force fields [95], the Sybyl/TINKER force fields [96, 97], the Charmm force fields [98, 99], the Discover force field [89, 100] and the empirical conformational energy program for peptides (ECEPP) force fields [101]. Each of these force fields has also undergone an evolutionary process, with all starting with simple harmonic terms for the bond and valence angles, Fourier series for the torsions and simple point charge electrostatic and van der Waals 6-12 (or 9) non-bonded terms. This simple functional form was used at the early stages both for its simplicity and also due to the problem of determining the parameters. As one adds complexity to the functional form, one also adds complexity to the parameterization scheme. Using a nonlinear least squares parameterization requires that one have data to use to determine the parameters. Originally only experimental data was used, but in the second and third generation force fields, *ab initio* data has been used in the parameterization, first RHF/6-31G\* data and subsequently MP2/6-31G\* and now Becke3LYP/6-31G\* data. As computers have gotten faster, the use of higher level theory has been used. Here one must be careful when one fits to *ab initio* data, in that the level of theory whose data one is using, actually accurately can determine the parameters one is trying to fit. A good example is using RHF and DFT data to determine the van der Waals parameters. This is not a good idea, since the dispersion energy is not accurately determined at either level of theory. Hence Hagler and coworkers have utilized experimental crystal data to determine these parameters. But then one has a problem in how to put the various parameters together, since some are determined by fitting to various levels of *ab initio* data and others are determined by fitting to various experimental data. Solvent reaction field models have also been implemented at the RHF and DFT levels of theory [102]. There has also been some debate on the recently derived polarizable force fields parameterized from *ab initio* calculations [103, 104].

### 7.3.6 Conformational States

The duplex consists of two chemically linked thymine nucleotides while the dimer consists of two thymine nucleotides linked by nonbonded forces, the so

called stacked dispersion interactions, which are not well treated by currently implementations of DFT, that is, pure GGA and the simple B3LYP hybrid. Note that Goddard has recently developed a new hybrid which treat dispersion as an exchange term correction, though many believe this to be purely a correlation effect. Note that in DFT the clear distinction between exchange and correlation is not always clear. With the use of the exact nonlocal Hartree exchange operator, this becomes clear. This is very important for the treatment of excited states, in addition to the treatment of dispersion. The one last term, the charge transfer effect, is also poorly treated in general by DFT. Hence the most accurate simulations for the benzene dimer which gets the attractive potential for the stacking dispersion interactions, as a CCSDTQ, which is clearly not feasible for the system we are treating in this work. The other alternative is to add a correction term to DFT as we have done in our work on LeuE (SCC-DFTB+Disp).

There are two distinct conformational states in the damaged DNA duplex which dominate. Hence it is important to have a spectroscopic probe which can distinguish between the two. Without this probe, one does not have a way to know how the DNA is damaged. Note that there are two distinct proteins for repair. Photolyase complex is involved with cyclobutane damaged duplex and which repairs the oxetane damaged duplex.

### **7.3.7 Vibrational spectroscopy from *ab initio* wave function and density functional theory (DFT) calculations**

Finally we would like to use vibrational spectroscopy as one of our main tools in both benchmarking and testing our various methods, but also in parameterizing and developing our methods. This has been done in the past, as vibrational frequencies have been used in determining vibrational force fields, that is, force fields used to predict the vibrational frequencies of molecules. Here the frequencies of small symmetrical molecules have been used to determine harmonic force constants which have then been transferred to larger molecules. But recently people in the molecular mechanics and molecular dynamics field have begun to interact with those in the vibrational force field field.



It was very early recognized that the vibrational frequencies predicted by the molecular mechanics force fields were of much lower accuracy than those predicted by vibrational force fields. One of the reasons was the methodology, functional form and data used by each group. On the basis of our DFT calculations of the dimer and duplex of thymine we have simulated the VA and Raman spectra as seen in [62]. This is in order to investigate the changes in electronic structure that UV radiation causes reflected in the changes in bonding as seen in these spectra. We can in a visual simulation see the characteristic modes and which internal coordinates these modes. In many cases the mode is a collective motion, that is, the excitation is clearly not localized.

### **7.3.8 *Ab initio* computational methods for nucleotides**

The computational methods which we have used are restricted Hartree-Fock, second order Møller Plesset theory (MP2) and density functional theory (DFT). In most of work we have utilized the 6-31G\* basis set. We also compare to results utilizing the AM1 and PM3 semi-empirical methods [63–65].

Ultra violet radiation, particularly in the range of 200 – 300 nm wavelength, irradiated on thymine in DNA, creates a dimerization attaching two of them, thereby creating a kink in the helical axis of DNA. This lesion perturbs the structure of DNA and leads to an error in the code and causing problems for the transcription [71, 72]. Under photo-reactivation in the visible and near UV region the defect is repaired, breaking the lesion and restoring the thymines back to the original state [73].

Density Functional Theory (DFT) calculations have been performed on several structures of thymine configurations. This was done in order to obtain optimized electronic structures of the atomic configurations of the important molecules participating in the UV damaging and subsequent repair processes. The central molecule to calculate is the one that is being damaged and then repaired. Therefore we chose first to calculate the various thymine configurations in the presence of the cofactor, riboflavin, and the phosphor-sugar DNA-backbone. Since the main question of the paper was the energy balance we would calcu-

late the energy of the thymine molecule in the various electronic states, *i.e.*, the ground state and the first excited state. Thus the basic task here was to calculate the electronic orbitals of the two different thymine systems, *i.e.*, the 2 thymine molecules separated and the duplex thymine molecule where the 2 pyrimidine rings are attached to each other. After calculating the configurations in the ground state we want to determine their energies in the ground state and first excited state. By filling up the electronic orbitals with electrons one can get an estimate of the energy of the highest occupied molecular orbital (HOMO) and the lowest unoccupied molecular orbital (LUMO) and then obtain the difference of those two energies, the HOMO-LUMO gap. Our hypothesis of the paper requires that this gap is sufficient to overcome for blue light and furthermore is much smaller than the energy barrier between the two di-thymine states. This was indeed what we found:

1. The energy of the HOMO-LUMO gap for separate di-thymine is 4.458 eV.
2. The energy of the HOMO-LUMO gap for attached di-thymine is 3.967 eV.
3. The energy barrier height between the ground state of the two di-thymine is 8.672 eV.

The last number was obtained from the estimate of the formation of the relevant attaching bonds. All energies were translated from Hartree to electron Volt energies. The results mentioned above suggest that the repair process when utilizing blue visible light will have to employ the excited state where the barriers are smaller than that of the ground state being around twice of what blue light can overcome in energy. The optimization in the DFT calculation was carried out with the 3BLYP methodology and within the DO gauge. The Gaussian 98 and 03 computer software packages were used for the calculation.

### **Nucleic acids (bases) in gas phase and isolated state**

Data in the gas phase or isolated state are rather limited for biological methods. But recently people have tried to perform more gas phase experiments on the nucleic acid bases, with the hopes of trying to understand the mechanism(s) of radiation damage [66, 67].

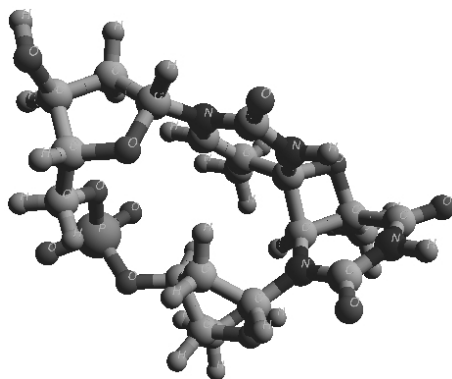


Figure 7.5. First dithymine dimer structure with oxetane damaged 4-membered ring

### 7.3.9 Nucleic acids in aqueous solution

The spectra of the nucleic acids in the aqueous phase must be carefully measured. This is due to the possible concerning uncontrolled pH, ionic strength, counter-ions, etc. In the following we discuss the energy and structure of the various oligomers of nucleic acids.

#### Relative energies, structures

The most important feature of proteins is their flexibility, as exemplified by the phi and psi backbone angles, which determine the secondary structure of proteins. As mentioned above, there are two main secondary structural elements prevailing in proteins, helices and beta sheets. But for small peptides there are many conformations which are possible. The relative energies of these various structures have been used exclusively as data for parameterization and also for testing.

In Figs. 7.5 and 7.6 we see the model for the dithymine dimer damaged by UV radiation. Finally to model the separate thymine molecules we have optimized the structure of two thymine molecules such that they can interact via base stacking as shown in Figure 7.7. This is also the case when one adds the phosphate backbone and ribose sugars. The reason that the damaged DNA structures be modelled at this level of theory is that the two thymine rings are connected via the chemical bonds within the oxetane and cyclobutane 4-membered ring

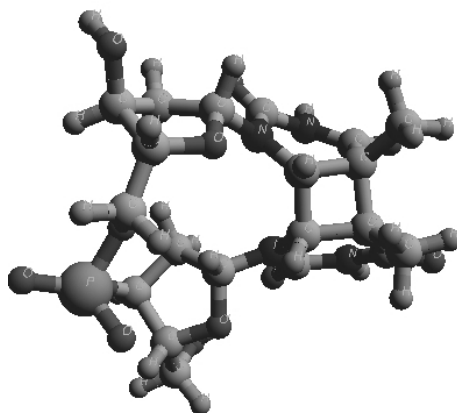


Figure 7.6. Second dithymine dimer structure with cyclobutane damaged 4-membered ring

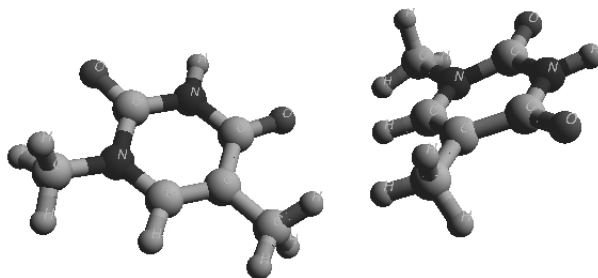


Figure 7.7. Third dithymine dimer structure, here without the phosphate backbone and ribose sugars

systems. As one can see the B3LYP hybrid exchange correlation functional is not optimal for these types of interactions. The Truhlar group has developed the MO5 and MO6 meta hybrid exchange correlation functionals to deal with such cases.

### 7.3.10 Case II: Electronic studies of processes in photosynthesis

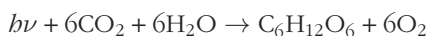
A study of electronic processes in the chlorophyll and carotenoid molecules of the photo-reaction center II is presented with the focus on the electronic excitations and charge transfer in the photosynthetic process. Several novel ideas are mentioned especially concerning the electron replenishment and nuclear vibrational excitations. For detailed information there are excellent reviews on

the matter both in proceedings [105–108] and in books or periodicals [105, 109, 110].

### 7.3.11 Introduction

The sun is the primary source of energy for almost all life on the earth and it supplies this energy in the full electromagnetic spectrum besides other radiation. The energy from the sunlight is supplied to the biosphere through the photosynthetic process, either directly (by incident photons) or indirectly (by climate changes, evaporation etc..) Needless to say, all organisms require energy for the chemical reactions of their life processes where chemical reactions are involved with reproduction, growth and maintenance.

Photosynthesis is the essential source of energy for plants that use solar energy to produce carbohydrates (glucose) to be stored in bonds for later needs of energy to the cell [108]. For animals the energy is supplied mostly by the reverse process of photosynthesis, respiration, although photo-radiation is important also as a secondary means. Below we give the fundamental chemical formulas for 1) photosynthesis and 2) respiration where water and carbondioxide (and light) in the former case is supplied while oxygen and glucose is the product opposite to the latter case where oxygen and glucose is supplied and where the products are water and carbondioxide. In a simple way, we can write the overall chemical reaction as:



Subsequently, we shall discuss these reactions in terms of the electronic structure of the atoms and molecules involved. Basically the will be a transfer of electrons along with a dissociation of water.

Plants receive light at daytime when the photosynthetic process is active but at night the metabolic processes basically become active, as an overall tendency [108].

The photosynthetic process is one of the most effective and sophisticated en-

ergy harvesting processes known in nature with a quantum efficiency of around 95% [111, 112] in getting photo-energy converted into electrical energy. Besides, there is the remarkable property of the molecules in photosynthesis that they are able to collect and transfer more than 99% of the collected solar energy to their reaction center [113, 114].

### **7.3.12 Bio-organisms using photosynthesis**

There are three types of organisms that use photosynthesis: Archaea, Bacteria, and Eucarya of which the last one is considered to be a higher level organisms. They all convert light into chemical free energy. The more primitive Archaea includes the halobacteria that also convert light into chemical energy but without oxidation/reduction chemistry and hence no use is made of CO<sub>2</sub> as a carbon source, *cf.* [108].

The higher photosynthetic organisms can be divided into oxygenic, photosynthetic organisms such as plants and algae and an-oxygenic photosynthetic organisms being certain types of bacteria. The former class has organisms that reduce CO<sub>2</sub> into carbohydrate by extraction of electrons from H<sub>2</sub>O yielding O<sub>2</sub> and H<sup>+</sup> while the latter class, believed to be more ancient, involves extraction of electrons from molecules other than water and without oxygen [109].

The process of photosynthesis in plants and algae is centered around certain organelles, the chloroplasts, which consists of a “light” reaction part involving transfer of electrons and protons and a “dark” reaction part that involves the biosynthesis of carbohydrates from CO<sub>2</sub> [108] also called carbon fixation.

We shall in this article mostly be concerned with the “light” reaction which occurs in a membrane system comprising proteins, electron carriers embedded in lipid molecules building up a membrane that divides the space into inner and outer domains and through which molecules or ions can pass. The protein complex, the light harvesting complex, gives a scaffold for the organic compounds, the chlorophylls and peridinin. The electron carriers are aromatic groups and metallic ion complexes. The protein complex controls the electron pathway entering the complex via an antenna molecule, peridinin or carotenoid, that ab-

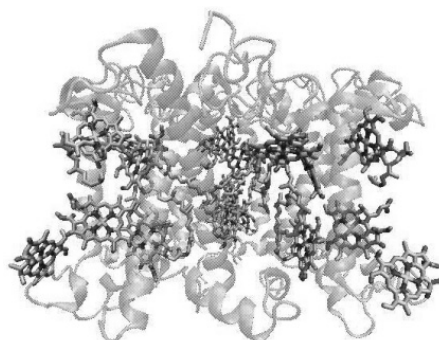
sorbs the photons and thereby causes the excitation of electrons. The electrons, or actually the charge displacements caused by the excitations, are then being transferred from one carrier to another.

### 7.3.13 The basic molecules of photosynthesis

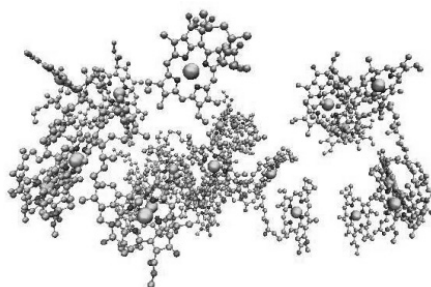
There are today crystallographic X-ray diffraction structures of the photosynthetic reaction center in the protein databases, *e.g.*, from the organism *Rhodospirillum rubrum* [117]. In Figure 7.8 the molecular system is illustrated. The center of the protein with ligands is anchored in the membrane and which, in the case of plants, are the chloroplasts anchored in the thylakoid membrane (the membrane containing light harvesting complex, electron transport chain and the ATP synthase). The small plackets in Figure 7.8 are the chlorophyll molecules that are the focus of the present study.

In Figure 7.8(b) the chlorophyll molecules from the light harvesting complex are arranged in a ring around the structure [118] where they receive incoming photons from peridinin or carotenoid [119]. We shall propose an overall picture of the processes involving photosynthesis that concerns chlorophyll and we shall present electronic pathways in support of that.

Basically, an incoming photon excites the antenna molecule and creates an exciton moving to the chlorophyll ring which acts as a storage ring consisting of 16 chlorophyll molecules arranged in asymmetric pairs of almost parallel plackets. Such a storage ring consisting of smaller rings can accumulate up to 8 electrons and reject bunches of 4 electrons that are carried away by certain proteins to another similar reaction center. This storage ring, or rather sink, is dependent on the nature of the excited states of the chlorophyll and carotenoid molecules and that, in turn, is very dependent on the excitation gap energy derived from the HOMO-LUMO value calculated in an energy-density functional theory. The ionization energy of the relevant quantum states can also be derived from this calculation as discussed later.



(a) Light Harvesting Complex



(b) Chlorophylls

Figure 7.8. (a) shows the pea light-harvesting complex at 2.5 Å resolution (PDB ID: 2BHW) [115]. The protein is represented as NewCartoon and the chlorophyll a/b using licorice. (b) shows the chlorophyll molecules from the crystal structure represented in licorice. The chlorophylls are organized in two ring structures, one upper and one lower. The figures were generated using the VMD program developed in the group of Professor Klaus Schulten at UIUC [116].

#### 7.3.14 Efficiency Dichotomy in electronic transfer mechanisms

A much studied process is that of the photo-absorption of the antenna molecules, peridinin or carotenoid [120, 121]. They can, upon the absorption of a photon, shuffell excitons between conjugated  $\pi$ -bonds. alternating double and single carbon bonds thereby creating excitons that can propagate down to the attached chlorophyll packet molecule. The direction of the propagation of the exciton is dependent on the dipole orientation of the peridinin or carotenoid molecule that points towards the chlorophyll molecule, it is attached to.

The transfer along the antenna and from the antenna to a chlorophyll packet and from one packet to another in the chlorophyll ring system is usually con-



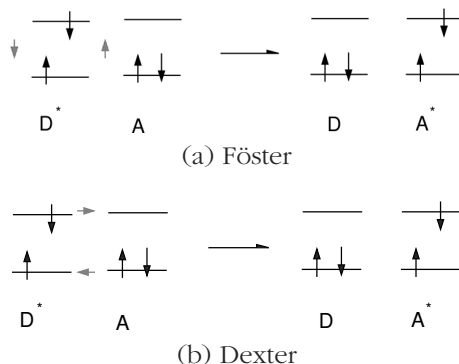


Figure 7.9. (a) illustrates the Förster mechanism where the excited electron is transferred due to dipole coupling. (b) illustrates the Dexter mechanism where an excited electron is transferred.

sidered to involve a Coulomb multipole-multipole interaction that de-excites an initially excited electron at a donor molecule and pass on this energy to directly excite an electron on the acceptor molecule and is usually called Förster mechanism [122]. Another way to de-excite the molecule is to transfer the energy to an adjacent molecule, known as the Dexter mechanism [123] and illustrated in Figure 7.9 and where an excited electron is exchanged for a ground state electron or a hole going oppositely (See Figure 7.9 for schematic illustration). In the latter case of transfer between different molecules we find it improbable that electrons are running between molecules like fixed entities. We shall instead propose that energy and excitation is transferred through electromagnetic interaction which is discussed in the next chapter. The purpose of this paper is to propose an interaction involved in causing both Förster and Dexter mechanism. That, namely a mechanism other than radiative transition is involved, is evident from the analysis of the efficiency factor. As mentioned, the proposed mechanism is responsible for a donor chromophore with electrons in excited states to be able to transfer energy by a long-range, non-radiative dipole-dipole interaction to another acceptor chromophore within a distance of about 10 nm. This remarkable mechanism is typically being used for resonance fluorescence phenomena [124] (or FRET, Fluorescence Resonance Energy Transfer) but in our case the focus is on chlorophyll molecules. The efficiency,  $E$ , of the mechanism

is often expressed in terms of the quantum yield of the energy transfer as

$$E = \frac{k_{\text{ET}}}{k_f + k_{\text{ET}} + \sum_i k_i} \quad (7.11)$$

where  $k_{\text{ET}}$  is the rate of energy transfer,  $k_f$  is the radiative decay rate and  $k_i$  is the rate constant for other de-excitation processes. In terms of the donor-acceptor separation distance  $a$  one can also write the efficiency  $E$  depending on the inverse 6<sup>th</sup> power law of  $a$ :

$$E = \frac{1}{1 + (a/a_0)^6} \quad (7.12)$$

where  $a_0$  is a normalization factor (separation of the donor-acceptor at which the resonance transfer is 50%) and is called the Förster distance. Even more interesting is that this distance,  $a_0$  is related to the overlap integral between the donor emission spectrum and the acceptor absorption spectrum along with the mutual molecular orientation. The overlap integral is expressed as

$$L = \int \epsilon_d(\nu)\alpha_a(\nu)\nu d\nu \quad (7.13)$$

where  $\epsilon_d$  and the  $\alpha_a$  are respectively the emission spectrum of the donor and the absorption spectrum (molar extinction coefficient) of the acceptor. This leads to a relation between the Förster distance and the overlap integral:

$$a_0^6 = 8.8 \times 10^{-28} \kappa^2 n^{-4} F_l L \quad (7.14)$$

$\kappa$  is the dipole orientation factor often set to  $\kappa^2 = 2/3$  [122].  $F_l$  is the fluorescence quantum yield of the donor in the absence of the acceptor and  $n$  is the refractive index of the medium.

Similar to the Förster mechanism of electron transfer (displacement) is the Dexter mechanism, which as described above involves both transfer of electron and hole and hence works predominantly on shorter distances. The formula for the efficiency of the Dexter mechanism is similar to the Förster that, however, has an  $1/a^6$  behavior rather than an exponential  $e^{-a}$  as in Dexter mechanism [123].

One can compare the radial behavior of the two mechanisms and at what distances they dominate. Basically Dexter dominates at distances  $a < 10 \text{ \AA}$  and

Förster mechanism at distances  $20 < a < 100 \text{ \AA}$  [125]. The Förster and the Dexter mechanisms help adding to (but not fully explain) the strong efficiency of the photosynthesis process with a total quantum efficiency of around 99%. The efficiency of the two mechanisms can also be expressed in terms of fluorescence lifetime of the donor molecule:

$$E = (1 - \tau_D^{ua}/\tau_D^a) \quad (7.15)$$

where  $\tau_D^a$  and  $\tau_D^{ua}$  are the fluorescence lifetimes of the donor state with and without the presence of an acceptor state. Such number is expected to be very low since the usual quantum yield or the fluorescence efficiency is given by the number  $n_{pe}$  of photons emitted divided by the number  $n_{pa}$  of photons absorbed, *i.e.*,

$$Q = \frac{n_{pe}}{n_{pa}} \quad (7.16)$$

which is a number close to 1. In the case of chlorophyll we expect the Förster and Dexter mechanisms to contribute much less than 100% [126] to the total quantum efficiency and thus, in order to explain this 99% quantum efficiency mentioned above we need another component which we shall explain in the next chapter.

### 7.3.15 The energy transfer mechanism in photosynthesis

We shall now try to formulate the entire photosynthesis process from a more abstract physical side. In such formulation the chloroplast is considered a whole molecular entity with chemical bonds and metal ions. In short our proposed process is as follows: *Basically, charges are being transferred around in the chloroplast system by the Coulomb interaction which can be expanded in multi-poles, the dipole part of which is responsible for Förster mechanism [122, 127]. However, we believe that there also appears to be electromagnetic interaction as a means of charge transfer and, most importantly, as a result of electron excitation that gives rise to nuclear vibration, which is in the far infrared region and to some extend verified in references [113, 114].*

As we argue, light being incident on a leaf with chlorophyll exhibits typical

resonant absorption peaks, particularly around 400 and 680 nm, see Refs. 113. The corresponding energy may be calculated using:

$$E = h\nu = 1.237 \times 10^3 \text{ eV}/\lambda(\text{nm}) \quad (7.17)$$

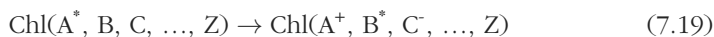
which leads, respectively, to 3.093 and 1.767 eV.

These energies could induce electronic excitations in many ligands chl(A, B, ..., Z) that are constituents of chlorophylls. Thus, symbolically one has



where Chl(A, B, C, ..., Z) stands for the electrons A, B, ...in the chlorophyll molecule, Chl, and A\* stands for excitation of electron A.

The electronic excitation could be Frank-Condon type or excimer type since electronic clouds of neighboring atoms overlap. In either case, the electronically excited state of one of the molecules can pass the electron to another one in excited state forming a kind of dipole. Before doing so, it could de-excite along the vibronic states emitting infrared radiation. Thus,



The electronically excited negative ion (C\*)<sup>-</sup> could de-excite to lower states leading ultimately to an isomeric state *i*, (C<sub>*i*</sub>)<sup>-</sup>. At this stage one has a dipole A<sup>+</sup>, ..., C<sub>*i*</sub><sup>-</sup>). The distance between two nuclei at this stage is affected and oscillates about their previous mean position, effectively creating **oscillating – dipoles**. This is supported by the experiments of Refs. 113, 114. In effect one has now a series of oscillating dipoles of dipole length *l* of about 2 to 3 Å or (0.2 to 0.3 nm). The components of electric field emitted by such an oscillating dipole in classical electrodynamics are [128] (z-axis is the axis of the dipole,  $\theta$  is with respect to that), for  $\lambda \gg l$ :

$$E_r = \frac{I_0 l}{4\pi} 2\eta \cos \theta \left[ \frac{1}{r^2} - \frac{i}{kr^3} \right] \exp(-ikr) \quad (7.20)$$

$$E_\theta = \frac{I_0 l}{4\pi} 2\eta \cos \theta \left[ \frac{ik}{r} + \frac{1}{kr^2} - \frac{i}{kr^3} \right] \exp(-ikr) \quad (7.21)$$

where  $\eta = \sqrt{\mu/\epsilon}$  ( $\mu$  is permeability in Henry/m and  $\epsilon$  is permittivity in Farad/m) which is the intrinsic impedance of the medium,  $k$ , the wave number =  $2\pi/\lambda$ ,  $\lambda$  being the wavelength radiated and  $I_0$  is the current.

Assuming that the current is uniform and  $q$  is the charge at the endpoints, in the frequency domain  $\omega$ , one can write  $I_0 = i\omega q$  and use  $\eta/k = (\omega\epsilon)^{-1}$ .

Then for the emitted radiation, with  $\lambda/2\pi \gg r$  we have:

$$E \cong \frac{ql}{4\pi\epsilon r^3} [2 \cos(\theta)\hat{e}_r + \sin(\theta)\hat{e}_\theta] \quad (7.22)$$

and in the same approximation:

$$H = \frac{I_0 l}{4\pi r^2} \sin(\theta)\hat{e}_\theta \quad (7.23)$$

The average Poynting vector,  $\langle S \rangle$ , is defined as  $\frac{1}{2}$  times the real part of the Poynting vector  $\mathbf{S} = (\mathbf{E} \times \mathbf{H})^*$ , so therefore, in terms of  $w/m^2$ :

$$\langle S \rangle = \frac{1}{8} \eta \sin^2 \theta \left( \frac{I_0 l}{\lambda r} \right) \hat{a}_r \quad (7.24)$$

and the total radiated power (in Watts),  $P$ , is thus:

$$P = 40\pi^2 I_0^2 \left( \frac{l}{\lambda} \right)^2 \quad (7.25)$$

In the case  $l \cong \lambda/1000$ ;  $P \cong (40\pi^2) I_0^2 \times 10^{-6}$  ( $I_0$  in Amps) then  $I_0 \approx q\nu$  where  $\nu$  is the frequency of vibration of 2 nuclei which can be estimated from vibrational spectra of one of the ligands. One can get this number from the vibrational spectra of aromatic molecules. The electric charge,  $q$ , is about  $1.602 \times 10^{-19}$  C for a single dipole. In the case of  $10^{20}$  dipoles per  $\text{cm}^3$ , this is a substantial energy.

Apart of the usual electron transfer mechanisms we have propose another electron transfer mechanism, the Bio-Auger process, that can replace or at least supplement the usually mentioned processes. In the figure below we have sketched the very interesting possibility of electrons being pumped to higher electronic energy states. This is because the electron that takes the place of the hole left from electron excitation by light absorption will deliver the extra energy gained from the hole replacement to the excited electron that has a higher

angular momentum state and thus cannot go back to the previous ground state position.

This boost or pumping of electrons are needed in order to cross from the carotenoid antenna molecule to the chlorophyll molecule that is at a much higher energy state. However the pumping of the excited electron can cause the crossing of the barrier between carotenoid and chlorophyll. the boosting is involving about 2 – 3 eV extra [129].

As mentioned earlier, the electronic transition caused by resonant absorption sets into motion a vibronic excitation due to the change of inter-nucleonic motion. This is in infrared frequencies. They are playing an important role contributing to the breaking up of water in the process where the manganese atoms in the center of the chloroplast play an important role of oxidation. The electromagnetic radiation is directed towards the center causing electron transports and oxidation as described above. The chlorophyll molecules are fixed in pairs (in a so-called  $C_2$  pseudo symmetry where each partner being rotated 180 degrees compared to the other). These pairs are then arranged almost in parallel around a ring (altogether 8 pairs) and will have electrons excited and de-excited arranged as a series of positive and negative charges working as a series of dipoles which effectively acts as capacitors adding up to the picture of chlorophyll molecules arranged as a storage ring of electrons. The issue here, from a theoretical solid-state point of view, is really how localized these kind of transfer mechanisms are in this “electron storage ring”. We expect that, after the electrons have been transferred to the chlorophyll ring they become de-localized and eventually be “spilled out” in portions of  $4e^-$  to the docking quinone-cytochrome molecule-complex to be carried away.

### **7.3.16 The structure and organization of chlorophyll**

The chlorophyll molecule is composed of a ring system with four nitrogens coordinating a magnesium ion and is part of the light harvesting complex. A single chlorophyll molecule, which is pictured in Figure 7.10, has a ring structure with 5 pyrine rings arranged inside the ring around a magnesium atom that

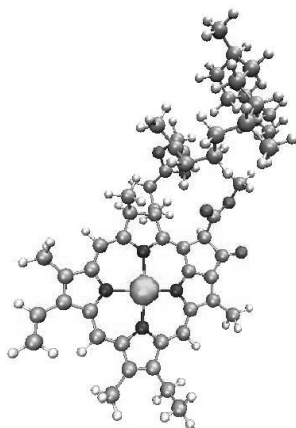


Figure 7.10. It shows the chlorophyll molecule where the green sphere is the  $Mg^{2+}$  coordinated by four nitrogen atoms (blue spheres). Carbon atoms are colored cyan, hydrogen white, and oxygens are colored red. Figure was generated using VMD.

coordinates to the neighboring nitrogens [117]. The tail of the molecule anchors to the protein complex.

The chlorophylls are arranged in two layers within the thylakoid membrane where each layer is located near either side of the membrane pointing toward the stromal or luminal surface. In each layer neighboring chlorophylls are located  $11.26 \text{ \AA}$  away from each other measured from the  $Mg^{2+}$  ion. These chlorophyll molecules are slightly asymmetric and are positioned in pairs of mirror images and arranged around a ring of 8 mirror image pairs. The molecules are located with a pseudo  $C_2$ -symmetry between each pair of chlorophylls [118].

### **Computation of chlorophyll analog**

We start by performing calculation of a single chlorophyll analog molecule where the tail of molecule has been removed resulting in 82 atoms. The main function of the tail is anchoring of the head group so for transfer properties it can be neglected. Tentatively we could calculate a HOMO-LUMO gap to be  $3 - 4 \text{ eV}$ . Such a HOMO (Highest Occupied Molecular Orbital) - LUMO (Lowest Un-occupied Molecular Orbital) is somewhat artificial in standard DFT formalism unless time-dependent methods are being used.

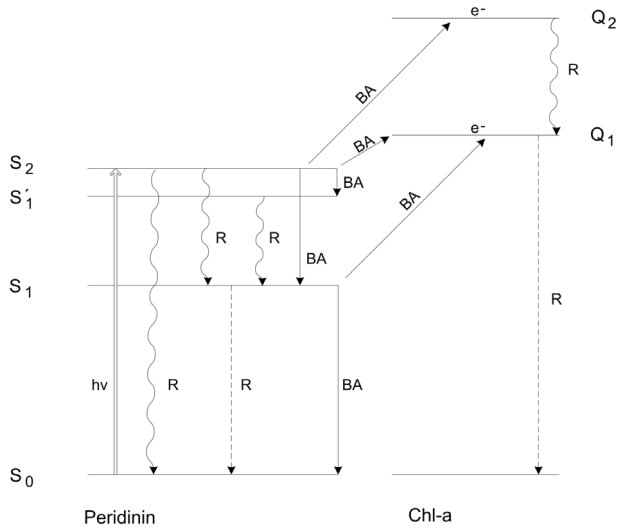


Figure 7.11. Schematic level scheme of peridinin-Chl-a complex. Thick arrow refers to the absorption of pigment from the ground state of peridinin,  $S_0$ , to the allowed state,  $S_2$ , the  $S_0 \rightarrow S_1$  being symmetry forbidden. Solid, broken and wavy lines refer, respectively, to Bio-Auger, fluorescence and allowed (dipole) radiative transitions. The case of the state  $Q_1$  is lower than  $S_1$  and  $S_2$ .

### 7.3.17 ESR experiments on the chloroplast system

To verify experimentally the assumptions made in the presented model, we arranged a preliminary experiment on chloroplast systems from plants in an ESR (Electron Spin Resonance) apparatus operated at low temperature. Thus we should, for example, be able to see if there was a difference in the signal from the unpaired electrons from day time with incident light and night time of no incident light. The most clear signal of electronic spin is expected to come from the manganese atoms. We have made recordings during specific periods (5 min. each) with incident full-spectral light and with no light at the sample cell situated in the magnet. One can observe a clear difference in the recording of the two types of periods.

In Figures 7.11 and 7.12 we have sketched examples of the Bio-Auger process. It shows schematically the transfer of electrons from peridinin to chlorophyll in the peridinin-chl-a complex. On the next figure the boosting of the



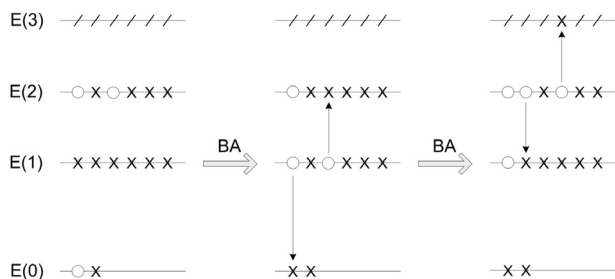


Figure 7.12. Schematic diagram exhibiting the upward boosting of an electron from a lower to higher energy states.

electron energy is illustrated by electron-hole examples.

## 7.4 Conclusions

A theory of the electronic pathways in the photosynthesis involving carotenoid and chlorophyll molecules has been proposed here. Upon exposure to incident light, the photo-excited carotenoid charge transfer electrons to carotenoid effectively creating an oscillating dipole. The chlorophyll molecules, arranged in a “storage” ring around a manganese atom, will transfer excitations of electrons alternating between  $\pi$  and  $\pi^*$  states exchanging quanta by a Förster-like mechanism that can account for 80-90% of the energy output. The rest is explained by EM radiation originating from nuclear vibrations.

## Acknowledgments

HGB would like to thank the Danish National Research Foundation for financial support and acknowledge the Danish Research Council for the funding of the Quantum Protein Centre in the Department of Physics at the Technical University of Denmark, 2800 Kgs. Lyngby, Denmark for the years 2001 to 2009. HGB would like to thank Karl James Jalkanen, FRSC, for many years of collaboration in the field of molecular biophysics and biospectroscopy, a long lasting friendship and for help in preparing this manuscript and finally Vladislav Vasilyev for developing the jamberoo program and making it available to the

computational molecular biophysics, quantum chemistry, computational physics and chemistry communities. The jamberoo program can be obtained at <http://sf.anu.edu.au/~vvv900/cct/appl/jmoleditor> and the citation for the program is <http://dx.doi.org/10.1007/s00214-009-0636-7> "Towards interactive 3D graphics in chemistry publications" *Theor. Chem. Acc.* **125**, 173-176 (2010).

## References

- [1] G. J. Thomas, Jr., *Ann. Rev. Bioph. Biom.* **28**, 1 (1999).
- [2] T. A. Keiderling, *Spectroscopic Methods For Determining Protein Structure in Solution* (VCH Publishers, Weinheim, 1996), "Protein Structural Studies Using Vibrational Circular Dichroism Spectroscopy", chap. 8, pp. 163.
- [3] G. J. Thomas, Jr., *Vibrational Spectra and Structure* (Elsevier, Amsterdam, 1975), "Raman Spectroscopy of Biopolymers", vol. 3, pp. 239.
- [4] K. J. Jalkanen, H. G. Bohr, and S. Suhai in *Proceedings of the International Symposium on Theoretical and Computational Genome Research*, edited by S. Suhai (Plenum, New York, 1997), pp. 255.
- [5] E. Tajkhorshid, K. J. Jalkanen, and S. Suhai, *J. Phys. Chem. B* **102**, 5899 (1998).
- [6] K. Frimand, K. J. Jalkanen, H. G. Bohr, and S. Suhai, *Chem. Phys.* **255**, 165 (2000).
- [7] K. J. Jalkanen, R. M. Nieminen, K. Frimand, J. Bohr, H. Bohr, R. C. Wade, E. Tajkhorshid, and S. Suhai, *Chem. Phys.* **265**, 125 (2001).
- [8] S. Abdali, K. J. Jalkanen, H. Bohr, S. Suhai, and R. N. Nieminen, *Chem. Phys.* **282**, 219 (2002).
- [9] K. J. Jalkanen, I. M. Degtyarenko, R. M. Nieminen, X. Cao, L. A. Nafie, F. Zhu, and L. D. Barron, *Theor. Chem. Acc.* **119**, 191 (2008).
- [10] M. Knapp-Mohammady, K. J. Jalkanen, F. Nardi, R. C. Wade, and S. Suhai, *Chem. Phys.* **240**, 63 (1999).
- [11] K. J. Jalkanen, R. M. Nieminen, M. Knapp-Mohammady, and S. Suhai, *Int. J. Quantum Chem.* **92**, 239 (2003).
- [12] Z. Deng, P. L. Polavarapu, S. J. Ford, L. Hecht, L. D. Barron, C. S. Ewig,

- and K. J. Jalkanen, *J. Phys. Chem.* **100**, 2025 (1996).
- [13] K. J. Jalkanen and S. Suhai, *Chem. Phys.* **208**, 81 (1996).
- [14] W.-G. Han, K. J. Jalkanen, M. Elstner, and S. Suhai, *J. Phys. Chem. B* **102**, 2587 (1998).
- [15] H. G. Bohr, K. J. Jalkanen, K. Frimand, M. Elstner, and S. Suhai, *Chem. Phys.* **246**, 13 (1999).
- [16] C.-D. Poon, E. T. Samulski, C. F. Weise, and J. C. Weisshaar, *J. Am. Chem. Soc.* **122**, 5642 (2000).
- [17] C. F. Weise and J. C. Weisshaar, *J. Phys. Chem. A* **107**, 3265 (2003).
- [18] M. Losada and Y. Xu, *Phys. Chem. Chem. Phys.* **9**, 3127 (2007).
- [19] R. D. Amos, *Chem. Phys. Lett.* **108**, 185 (1984).
- [20] P. J. Stephens, *J. Phys. Chem.* **89**, 748 (1985).
- [21] P. J. Stephens, *J. Phys. Chem.* **91**, 1712 (1987).
- [22] A. D. Buckingham, P. W. Fowler, and P. A. Galwas, *Chem. Phys.* **112**, 1 (1987).
- [23] R. D. Amos *Adv. Chem. Phys.: Ab Initio Methods in Quantum Chemistry*, edited by K. P. Lawley (Wiley, Chichester, 1987), "Molecular property derivatives", chap. 2, vol. 67, pp. 99.
- [24] R. D. Amos, K. J. Jalkanen, and P. J. Stephens, *J. Phys. Chem.* **92**, 5571 (1988).
- [25] R. M. Stevens, R. M. Pitzer, and W. N. Lipscom, *J. Chem. Phys.* **38**, 550 (1962).
- [26] J. R. Cheesman, M. J. Frisch, F. J. Devlin, and P. J. Stephens, *Chem. Phys. Lett.* **252**, 211 (1996).
- [27] D. P. Craig and T. Thirunamachandran, *Mol. Phys.* **35**, 825 (1978).
- [28] P. J. Stephens, K. J. Jalkanen, R. D. Amos, P. Lazzeretti, and R. Zanasi, *J. Phys. Chem.* **94**, 1811 (1990).
- [29] K. L. Bak, P. Jørgensen, T. Helgaker, K. Ruud, and H. J. Aa. Jensen, *J. Chem. Phys.* **98**, 8873 (1993).
- [30] K. L. Bak, P. Jørgensen, T. Helgaker, K. Ruud, and H. J. Aa. Jensen, *J. Chem. Phys.* **100**, 6621 (1994).

- [31] A. Komornicki and J. W. McIver, *J. Chem. Phys.* **70**, 2014 (1979).
- [32] R. D. Amos, *Chem. Phys. Lett.* **124**, 376 (1986).
- [33] M. J. Frish, Y. Yamaguchi, J. F. Gaw, H. F. Schaefer III, and J. S. Binkley, *J. Chem. Phys.* **84**, 531 (1986).
- [34] B. G. Johnson and J. Florian, *Chem. Phys. Lett.* **247**, 120 (1995).
- [35] R. D. Amos, *Chem. Phys. Lett.* **87**, 23 (1982).
- [36] T. Helgaker, K. Ruud, K. L. Bak, P. Jørgensen, and J. Olsen, *Faraday Discuss.* **99**, 165 (1994).
- [37] J. R. Cheeseman, M. J. Frisch, F. J. Devlin, and P. J. Stephens, *J. Phys. Chem. A.* **104**, 1039 (2000).
- [38] P. J. Stephens, F. J. Devlin, J. R. Cheeseman, and M. J. Frisch, *J. Phys. Chem. A.* **105**, 5356 (2001).
- [39] P. J. Stephens, F. J. Devlin, J. R. Cheeseman, M. J. Frisch, B. Mennucci, and J. Tomasi *Tetrahedron: Asymmetr.* **11**, 2443 (2000).
- [40] J. E. Rice and N. C. Handy, *J. Chem. Phys.* **94**, 4959 (1991).
- [41] S. M. Colwell, C. W. Murray, N. C. Handy, and R. D. Amos, *Chem. Phys. Lett.* **210**, 261 (1993).
- [42] A. M. Lee and S. M. Colwell, *J. Chem. Phys.* **101**, 9704 (1994).
- [43] S. J. A. van Gisbergen, J. G. Snijders, and E. J. Baerends, *J. Chem. Phys.* **103**, 9347 (1995).
- [44] S. J. A. van Gisbergen, J. G. Snijders, and E. J. Baerends, *Chem. Phys. Lett.* **259**, 599 (1996).
- [45] S. J. A. van Gisbergen, K. Kootstra, P. R. T. Schipper, O. V. Gritsenko, J. G. Snijders, and E. J. Baerends, *Phys. Rev. A* **57**, 2556 (1998).
- [46] S. J. A. van Gisbergen, J. G. Snijders, and E. J. Baerends, *J. Chem. Phys.* **109**, 10644 (1998).
- [47] S. J. A. van Gisbergen, J. G. Snijders, and E. J. Baerends, *J. Chem. Phys.* **109**, 10657 (1998).
- [48] K. J. Jalkanen, P. J. Stephens, R. D. Amos, and N. C. Handy, *J. Phys. Chem.* **92**, 1781 (1988).
- [49] A. D. Becke, *J. Chem. Phys.* **98**, 5648 (1993).

- [50] A. D. Becke, *J. Chem. Phys.* **96**, 2155 (1992).
- [51] A. D. Becke, *J. Chem. Phys.* **97**, 9173 (1992).
- [52] A. D. Becke, *J. Chem. Phys.* **88**, 1053 (1988).
- [53] C. Lee, W. Yang, and R. G. Parr, *Phys. Rev. B* **37**, 785 (1988).
- [54] S. H. Vosko, L. Wilk, and M. Nusair, *Can. J. Phys.* **58**, 1200 (1980).
- [55] K. Holderna-Natkaniec, K. Jurga, I. Natkaniec, D. Nowak, and A. Szyzewski, *Chem. Phys.* **317**, 178 (2005).
- [56] M. R. Johnson, M. Prager, H. Grimm, M. A. Neumann, G. J. Kearley, and C. C. Wilson, *Chem. Phys.* **244**, 49 (1999).
- [57] B. S. Hudson, *J. Phys. Chem. A*, **105**, 3949 (2001).
- [58] T. B. Freedman, *Faraday Discuss.* **199**, 210 (1994).
- [59] P. L. Polavarapu, *Faraday Discuss.* **199**, 210 (1994).
- [60] P. L. Polavarapu and Z. Deng, *Faraday Discuss.* **99**, 151 (1994).
- [61] R. J. Bartlett, I. V. Schweigert, and V. F. Lotrich, *J. Mol. Struct.: THEOCHEM*, **771**, 1 (2006).
- [62] K. J. Jalkanen, Jürgensen, V.W., A. Claussen, A. Rahim, G. M. Jensen, R. C. Wade, F. Nardi, C. Jung, I. M. Degtyarenko, R. M. Nieminen, F. Herrmann, M. Knapp-Mohammady, T. A. Niehaus, K. Frimand and S. Suhai, *Int. J. Quantum Chem.*, **106**, 1160 (2006).
- [63] J. S. Dewar, Z. Ziegler, E. F. Healy, and J. J. P. Stewart, *J. Am. Chem. Soc.* **107**, 3902 (1985).
- [64] J. J. P. Stewart, *J. Comp. Chem.*, **10**, 209 (1989).
- [65] J. J. P. Stewart, *J. Comp. Chem.* **10**, 221 (1989).
- [66] S. Gohlke and E. Illenberger, *Europhysics News* **33**, 207 (2002).
- [67] S. D. Wetmore, R. Boyd, and L. A. Erikson, *Chem. Phys. Lett.*, **322**, 129 (2000).
- [68] R. Kakkar, and R. Garg, *J. Mol. Struct.: THEOCHEM* **620**, 139 (2003).
- [69] M. S. Cheung, I. Daizadeh, A. A. Stuchebrukhov, and P. F. Heelis, *Biophys. J.* **76**, 1241 (1999).
- [70] D. Ramaiah, Y. Kan, T. Koch, H. Ørum, and G. B. Schusgter, *P. Natl. Acad. Sci. USA* **95**, 12902 (1998).

- [71] W. Harm, *Biological Effects of Ultraviolet Radiation* (Cambridge University Press, Cambridge, 1980).
- [72] I. Husain, J. Griffith and A. Sancar, P. Natl. Acad. Sci. USA **85**, 2558 (1988).
- [73] A. Sancar and C. S. Rupert, Gene **4**, 295 (1978).
- [74] R. P. Sinha and D.-P. Hüder, Photochem. Photobiol. Sci. **1**, 225 (2002).
- [75] A. Sancar, Chem. Rev. **103**, 2203 (2003).
- [76] A. Reuther, D. N. Nikogosyan and A. Laubereau, J. Phys. Chem. **100**, 5570 (1996).
- [77] A. Sancar, Biochemistry **33**, 2 (1994).
- [78] H. Bohr, J. K. Jalkanen and J. B. Malik, Mod. Phys. Lett. B **19**, 473 (2005).
- [79] P. F. Heelis, J. Photoch. Photobiol. B **38**, 31 (1997).
- [80] T. Carell, L. T. Burgdorf, L. M. Kundu, and M. Cichon, Curr. Opin. Chem. Biol. **5**, 491 (2001).
- [81] G. B. Sancar, Mutat. Res. **451**, 25 (2000).
- [82] A. Kelner, P. Natl. Acad. Sci. USA **35**, 73 (1949).
- [83] A. Kelner, J. Bacteriol. **58**, 511 (1949).
- [84] R. Dulbecco, Nature **163**, 949 (1949).
- [85] M. Elstner, *Weiterentwicklung quantenmechanischer Rechenverfahren fuer organische Molekuele und Polymere*. PhD thesis (Universitaet-Gesamthochschule Paderborn, Deutschland, 1998).
- [86] M. Elstner, D. Porezag, G. Jungnickel, J. Elsner, M. Haugk, Th. Frauenheim, S. Suhai, and G. Seifert, Phys. Rev. B **58**, 7260 (1998).
- [87] T. Heine, *Die Berechnung von Structur, Energetik und kernmagnetischen Abschirmungen von Fullerenen und ihren Derivatzen*. PhD thesis (Technische Universitat Dresden, Germany, 2000).
- [88] K. Frimand and K. J. Jalkanen, Chem. Phys. **279**, 161 (2002).
- [89] J. R. Maple, M.-J. Hwang, K. J. Jalkanen, T. P. Stockfish, and A. T. Hagler J. Comp. Chem. **19**, 430 (1998).
- [90] S. J. Weiner, P. A. Kollman, Nguyen, D.T., and D. A. Case, J. Comp. Chem. **7**, 230 (1986).
- [91] S. J. Weiner, P. A. Kollman, D. A. Case, U. C. Singh, C. Ghio, G. Alagona,

- S. Profeta Jr., and P. Weiner, *J. Am. Chem. Soc.* **106**, 765 (1984).
- [92] C. H. Langley, J.-H. Lii, and N. L. Allinger, *J. Comp. Chem.* **22**, 1396 (2001).
- [93] H. Yu, T. Hanson, and W. F. van Gunsteren, *J. Chem. Phys.* **118**, 221 (2003).
- [94] W. R. P. Scott, P. H. Huenenberger, I. G. Tironi, A. E. Mark, S. R. Billeter, J. Fennen, A. E. Torda, T. Huber, P. Krueger, and W. F. van Gunsteren, *J. Phys. Chem.* **103**, 3596 (1999).
- [95] W. L. Jørgensen and J. Tirado-Rives, *J. Am. Chem. Soc.* **110**, 1657 (1988).
- [96] P. Ren and J. W. Ponder, *J. Comp. Chem.* **23**, 1497 (2002).
- [97] M. Clark, R. D. Cramer III, and N. van Opdenbosch, *J. Comp. Chem.* **10**, 982 (1989).
- [98] A. D. J MacKerell, D. Bashford, M. Bellott, J. R. L. Dunbrack, J. D. Evanseck, M. J. Field, S. Fisher, J. Gao, Guo, H., S. Ha, D. Joseph-McCarthy, L. Kuchnir, K. Kucyera, F. T. K. Lau, C. Mattos, S. Michnick, T. Ngo, D. T. Nguyen, B. Prodhom, W. E. Reiher III, B. Roux, M. Schlenkrich, J. C. Smith, R. Stote, J. Straub, M. Watanabe, J. Wiorkiewicz-Kuczera, D. Yin, and M. Karplus, *J. Phys. Chem. B.* **102**, 3586 (1998).
- [99] B. R. Brooks, R. E. Bruccoleri, B. D. Olafson, D. J. States, S. Swaminathan, and M. Karplus, *J. Comp. Chem.* **4**, 187 (1983).
- [100] D. McKay, A. T. Hagler, J. R. Maple, and C. Herd, *Discover User's Guide* (Biosym Technologies (MSI) Inc., San Diego, 1991).
- [101] M. Vasquez, G. Nemethy, and H. A. Scheraga, *Macromolecules* **16**, 1043 (1983).
- [102] L. Jensen, P. Th. van Duijnen, and J. G. Snijders, *J. Chem. Phys.* **118**, 514 (2003).
- [103] G. Tabacchi, C. J. Mundy, J. Hutter, and M. Parrinello *J. Chem. Phys.* **117**, 1416 (2002).
- [104] R. Chelli and P. Procacci *J. Chem. Phys.* **118**, 1571 (2003).
- [105] J. Ames, *Photosynthesis* (Elsevier, Amsterdam, 1987).
- [106] *The Photosystems: Structure, Function and Molecular Biology*, edited by

- J. Barber (Elsevier, Amsterdam, 1992).
- [107] *Photosynthesis and the Environment*, edited by J. Barber (Kluwer Academic, Dordrecht, 1996).
- [108] J. Whitmarsh and Govindjee, *Concepts in Photobiology: Photosynthesis and photomorphogenesis*, edited by G. S. Singhal, G. Renger, S. K. Sopory, K.-D. Irrgang and Govindjee (Narosa, New Delhi, 1999), chap. "The photosynthetic process", pp 11.
- [109] P. H. Raven and G. B. Johnson, *Biology* (William C. Brown, Duxbury, 1996),
- [110] P. R. Chitnis, *Annu. Rev. Plant Phys.* **52**, 593 (2001).
- [111] R. J. Sension, *Nature*, **446**, 740 (2007).
- [112] G. S. Engel, T. R. Calhoun, E. L. Read, T.-K. Ahn, T. Mancal, Y.-C. Cheng, R. E. Blankenship, and G. R. Fleming, *Nature* **446**, 782 (2007).
- [113] T. Brixner, J. Stenger, M.H. Vaswani, M. Cho, R. E. Blankenship, and G. R. Fleming, *Nature* **434**, 625 (2005).
- [114] C. Day, *Phys. Today* **58**, 23 (2005).
- [115] J. Standfuss, A. C. T. van Scheltinga, M. Lamborghini, and W. Kühlbrandt, *Embo.J.* **24**, 919 (2005).
- [116] W. Humphrey, A. Dalke, and K. Schulten, *J. Mol. Graph.* **14**, 33 (1996).
- [117] J. Koepke, X. Hu, C. Muenke, K. Schulten, and H. Michel, *Structure* **4**, 581 (1996).
- [118] Z. Liu, H. Yan, K. Wang, T. Kuang, J. Zhang, L. Gui, X. An, and W. Chang, *Nature* **428**, 287 (2004).
- [119] A. Damjanovic, T. Ritz, and K. Schulten, *Phys. Rev. E*, **59**, 3293 (1999).
- [120] H. M. Vaswani, N. E. Holt, and G. R. Fleming, *Pure Appl. Chem.*, **77**, 925 (2005).
- [121] D. Zigmantas, T. Polivka, R. G. Hiller, A. Yartsev, and V. Sundström, *J. Phys. Chem. A* **105**, 10296 (2001).
- [122] Th. Förster, *Ann. Phys. (Leipzig)* **2**, 55 (1948).
- [123] D. L. Dexter *J. Chem. Phys.* **21**, 836 (1963).
- [124] J. R. Lakowicz, *Principle of Fluorescence Spectroscopy*. (Springer, Heidel-



- berg, 2006).
- [125] P. Andrew and W. L. Barnes, *Science* **306**, 1002 (2004).
- [126] V. Sundström, T. Pullerits, and R. van Grondelle, *J. Phys. Chem. B* **103**, 2327 (1999).
- [127] G. Cinque, R. Croce, A. Holzwarth, and R. Bassi, *Biophys. J.* **79**, 1706 (2000).
- [128] K. R. Demarest, *Engineering Electromagnetics* (Prentice Hall, NJ, 1998), chap. 14, p. 576.
- [129] H. Bohr and F. B. Malik, *Handbook of Molecular Biophysics* (Wiley-VCH, 2009), edited by H. Bohr, pp. 67.